Sima Sahu, Harsh Vikram Singh, Basant Kumar and Amit Kumar Singh*

A Bayesian Multiresolution Approach for Noise Removal in Medical Magnetic Resonance Images

https://doi.org/10.1515/jisys-2017-0402 Received August 6, 2017; previously published online January 10, 2018.

Abstract: A Bayesian approach using wavelet coefficient modeling is proposed for de-noising additive white Gaussian noise in medical magnetic resonance imaging (MRI). In a parallel acquisition process, the magnetic resonance image is affected by white Gaussian noise, which is additive in nature. A normal inverse Gaussian probability distribution function is taken for modeling the wavelet coefficients. A Bayesian approach is implemented for filtering the noisy wavelet coefficients. The maximum likelihood estimator and median absolute deviation estimator are used to find the signal parameters, signal variances, and noise variances of the distribution. The minimum mean square error estimator is used for estimating the true wavelet coefficients. The proposed method is simulated on MRI. Performance and image quality parameters show that the proposed method has the capability to reduce the noise more effectively than other state-of-the-art methods. The proposed method provides 8.83%, 2.02%, 6.61%, and 30.74% improvement in peak signal-to-noise ratio, structure similarity index, Pratt's figure of merit, and Bhattacharvya coefficient, respectively, over existing well-accepted methods. The effectiveness of the proposed method is evaluated by using the mean squared difference (MSD) parameter. MSD shows the degree of dissimilarity and is 0.000324 for the proposed method, which is less than that of the other existing methods and proves the effectiveness of the proposed method. Experimental results show that the proposed method is capable of achieving better signal-to-noise ratio performance than other tested de-noising methods.

Keywords: Modeling of wavelet coefficients, MRI image, de-noising, Bayesian estimator.

1 Introduction

During the acquisition process, noise affects the magnetic resonance (MR) image and de-noising is required because clinical diagnosis accuracy depends on the visual quality of the MR image. MR imaging (MRI) provides detailed images of organs and tissues in the human body. MRI is generally affected by random noise during the reconstruction process. Artifacts due to scanned object, magnetic susceptibility, radiofrequency coil, eddy current, pulse sequence design, and rigid and non-rigid motions are the sources of noise in MRI [26, 33, 34, 41]. The scanned object in the acquisition process causes thermal noise in MRI [31]. The noise in MRI can be Gaussian distributed or Rician distributed, depending on the reconstruction process of MRI [37]. The acquisition system of MR images can be a series or parallel acquisition system. A series acquisition system works in single-coil technology, while a parallel acquisition system works in multiple-coil technology. Single-coil technology introduces Rician distribution of noise, and multiple-coil technology introduces zero mean complex additive Gaussian noise with equal variance $(\sigma_{\rm c}^2)$ in each coil [19].

Sima Sahu: Dr. A. P. J. Abdul Kalam Technical University, Lucknow, Uttar Pradesh, India

Harsh Vikram Singh: Department of Electronics Engineering, Kamla Nehru Institute of Technology, Sultanpur, Uttar Pradesh, India Basant Kumar: Department of Electronics and Communications Engineering, Motilal Nehru National Institute of Technology, Allahabad, India

^{*}Corresponding author: Amit Kumar Singh, Department of Computer Science and Engineering, Jaypee University of Information Technology, Waknaghat, Solan, Himachal Pradesh, India, e-mail: amit_245singh@yahoo.com

Noise in MRI may be reduced by acquiring the data several times and averaging them. This method takes more acquisition time, and for that reason de-noising methods are preferred. A variety of studies on de-noising MR images have been published in the literature. The de-noising methods can be classified as a filtering approach, transform domain approach, and statistical approach [31]. Filters like spatial filters [30], non-local mean filters [28], bilateral filters [20], and anisotropic diffusion filters [24] are filtering approach filters. Filtering using wavelet transform [22], curvelet transform [7], and contourlet transform [3] are transform domain approach filtering methods. Filters based on statistical modeling and estimation methods like the maximum a posteriori (MAP) approach, maximum likelihood estimator (MLE) approach, and minimum mean square error (MMSE) approach come under statistical approaches.

De-noising using wavelet filters based on the multiresolution approach is more popular than the spatial domain and frequency domain filters. Wavelet filters decompose the noisy image into sub-bands at various levels. The signal components are estimated using thresholding (hard and soft) techniques. Neigh Shrink, Visu Shrink, Bayes Shrink, and Sure Shrink are popular wavelet de-noising methods. Wu et al. [39] proposed a wavelet-based de-noising filter for MR images. Anand and Sahambi [2] presented a de-noising method based on wavelet-based bilateral filtering for MR images. De-noising with complex wavelet transform was proposed by Zaroubi and Goelman [40]. An adaptive multiscale thresholding was proposed by Bao and Zhang [5] to de-noise MR images. Gai et al. [16] proposed a new multiscale-based de-noising algorithm. The de-noising algorithm is based on hidden Markov tree model utilizing the quaternion wavelet transform.

De-noising based on the statistical approach has been promising, as the de-noising efficiency depends on the correct estimation of noise and signal variances by use of estimators. The MLE-based de-noising approach was proposed by Sijbers and Den Dekker [36] for estimation of Rician noise level and de-noising MR images. A linear MMSE-based filter was proposed by Krissian and Aja-Fernandez [24] for filtering MRI for Rician noise. A wavelet-based median absolute deviation (MAD) estimator was developed by Coupe et al. [13] for estimating and de-noising MR images. He and Green Shields [21] proposed a post-acquisition de-noising method for MRI, using non-local maximum likelihood estimation (NLME). The authors proved that NLME performs better than MLE. Manjon et al. [29] proposed a de-noising method for removing both Rician and Gaussian distributed noise from MR images. They implemented a non-local noise estimation method, which adjusts the de-noising strength of the filter to remove the spatially varying noise present in the MR image. A homomorphic approach was proposed by Aja-Fernandez et al. [1] to reduce spatially variant noise in MR images. Rajan et al. [33] designed an NLME based on the Kolmogorov-Smirnov test to remove Rician noise from MR images. The method is an improvement over the NLME estimated method, based on the Euclidian distance. Awate and Whitaker [4] proposed a Bayes estimator for de-noising MR images. Gai et al. [17] developed a color image de-noising method based on color monogenic wavelet transform. The authors applied trivariate Gaussian distribution to capture the statistical dependencies between the wavelet coefficients and further used the MAP estimator to derive the shrinkage filter. In Ref. [14], the authors proposed an image denoising algorithm using an improved sparse representation in three-dimensional (3D) transform domain. The performance of the algorithm highly depends on the effective patch size/block. The algorithm estimates the codes of the overlapping patches and averages the estimates. Reconstruction of the patches by finding similar ones in the image is known as block matching. Further, the patches are stacked into 3D blocks and de-noised using hard thresholding and a Wiener filter.

In this study, the proposed method combined the features of wavelet transform and Bayesian estimator to remove additive and signal-independent noise. This method utilizes the properties of wavelet coefficient: that they are independent and identically distributed [12]. It is assumed that the wavelet coefficients are random variables and distributed by a probability density function (PDF). An appropriate PDF is required for effective modeling of the wavelet coefficients. The Bayesian approach estimator utilizes the PDF to obtain noise-free wavelet coefficients. Further, the proposed method utilizes the normal inverse Gaussian PDF for modeling wavelet coefficients. Our method is based on statistical modeling of wavelet coefficients, and it is applied for medical images. The effectiveness of the proposed method highly depends on the correct choice of PDFs.

Therefore, the proposed de-noising method is totally different from the method proposed in Ref. [14].

2 Background

2.1 Wavelet Transform and Statistical Modeling of Coefficients

Wavelet transform effectively performs image de-noising by converting image information into transform coefficients. Wavelet transform based on thresholding performs de-noising by retaining the large coefficients and setting others to zero [23]. The de-noising accuracy of the technique depends on the correct choice of the threshold value. In this paper, the authors attempt to find the threshold value by modeling the wavelet coefficients.

The application of wavelet transform converts the image into four sub-bands, namely approximation, horizontal, vertical, and diagonal sub-bands.

Let x(i, j) be the (i, j)th pixel in an MR image, corrupted by additive Gaussian noise n(i, j), resulting in noisy image y(i, j).

The noisy image can be expressed as

$$y(i,j) = x(i,j) + n(i,j).$$
 (1)

The PDF of additive noise is given by

$$p_n(n) = \left(\frac{1}{\sqrt{2\pi\sigma_n^2}}\right) e^{\left(\frac{-n^2}{2\sigma_n^2}\right)},\tag{2}$$

where, σ_n^2 is the variance of noise.

Wavelet transform up to m level converts the image into the LLm, LHk, HLk, and HHk sub-bands [27]. The LLm sub-band contains the low-frequency information of the image, which possesses most of the information. Discrete wavelet transform (DWT) has the capability to describe the local features either spectrally or spatially. This feature makes DWT perform de-noising while preserving corners and edges. The wavelet-transformed image can be written as

$$y_k^l(i,j) = x_k^l(i,j) + n_k^l(i,j),$$
 (3)

where l=1, 2, 3; k=1, 2, ... m; l=1; corresponds to horizontal orientation; l=2 corresponds to vertical orientation; l=3 corresponds to diagonal orientation; and $y_k(i,j), x_k(i,j)$ and $n_k(i,j)$ are the (i,j)th wavelet coefficients of y(i,j), x(i,j), and n(i,j), respectively, at level k. Figure 1 shows the wavelet decomposition of the MRI into level 3.

The distribution of wavelet coefficients is peaked at zero and has a heavy tailed structure [27], as shown in Figure 2. NIG PDF fits heavy-tailed data and is analytically tractable [11]. NIG PDF has been implemented in modeling of wavelet coefficients and results in effective noise reduction [8, 9]. The NIG distribution is the mixed distribution of normal distribution and inverse Gaussian distribution. NIG distribution defines a homogeneous Levy-type process [6]. The proposed NIG prior is defined as

$$p_{\nu}(x) = \alpha \delta e^{\alpha \delta} k_{\nu} (\alpha \sqrt{\delta^2 + x^2}) / \pi \sqrt{\delta^2 + x^2}, \tag{4}$$

where k is the modified Bessel function with j (index) = 1 and δ , α are the parameters. α defines tail heaviness and the steepness of the distribution can be controlled by it. δ defines the scale parameter [9].

The steepness of the NIG distribution curve increases with α . For heavier tails, a small value of α is preferred. When $\alpha \to \infty$ and $\delta \to \infty$, the NIG distribution results in Gaussian distribution. When $\alpha \to 0$, the NIG PDF converts to a Cauchy distribution [9].

Figure 3 shows that the NIG distribution fits better than the Gaussian (normal) distribution. The empirical distribution of wavelet coefficients in sub-band LL at level 1 and the corresponding fitting of NIG distribution are shown in Figure 4. The HH sub-band contains the most noise information. Thus, a Gaussian distribution can perfectly model the wavelet coefficients in the HH sub-band. The empirical cumulative distribution of

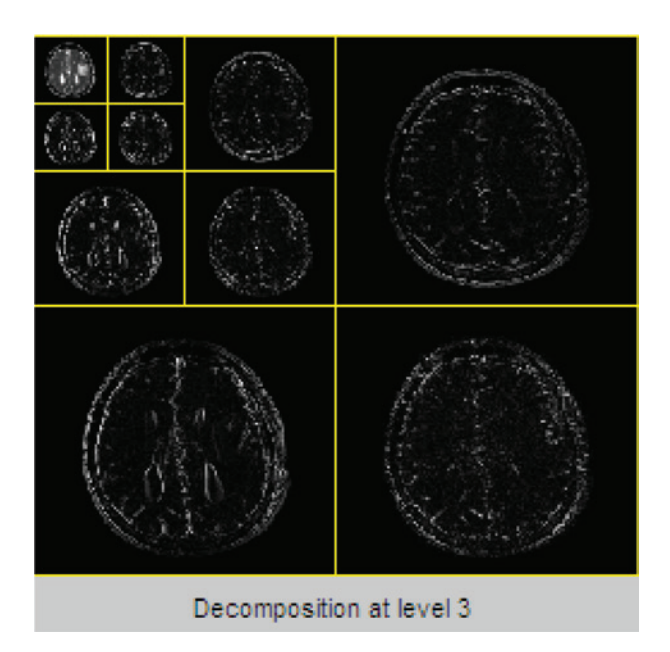


Figure 1: Three-Level Wavelet Decomposition of MR Image.

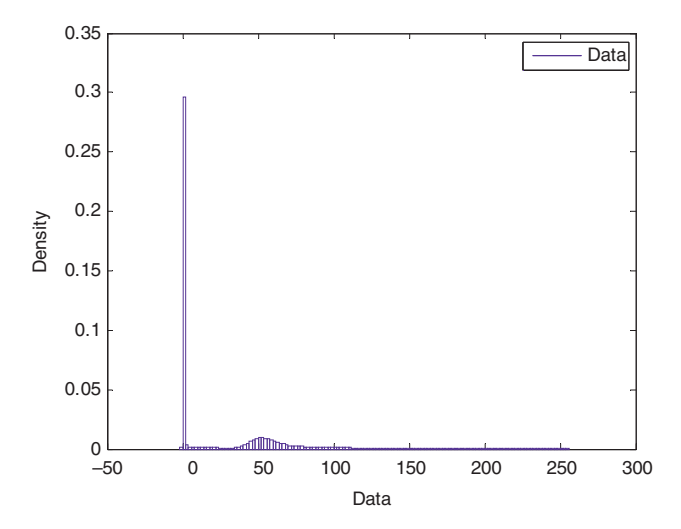


Figure 2: Distribution of Wavelet Coefficients.

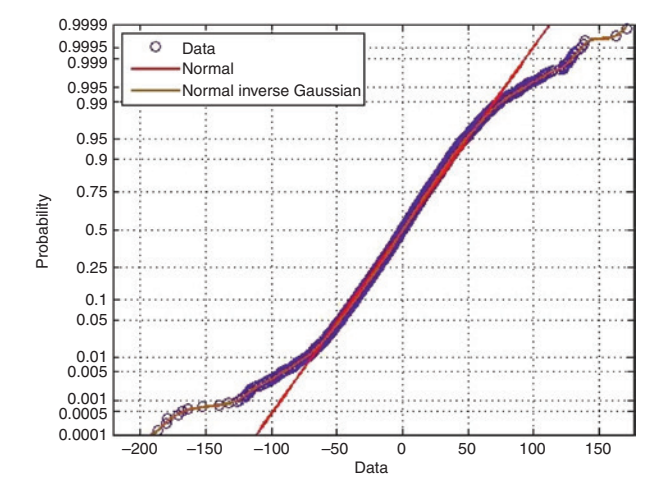


Figure 3: Probability Plot for MRI Data.

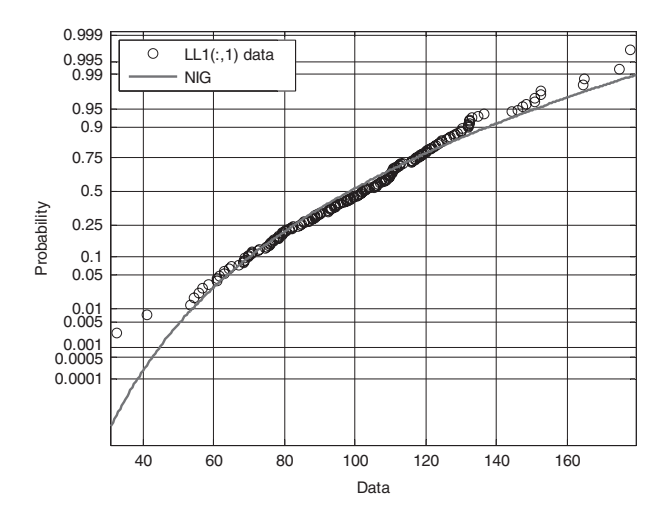


Figure 4: Probability Plot for LL Sub-band.

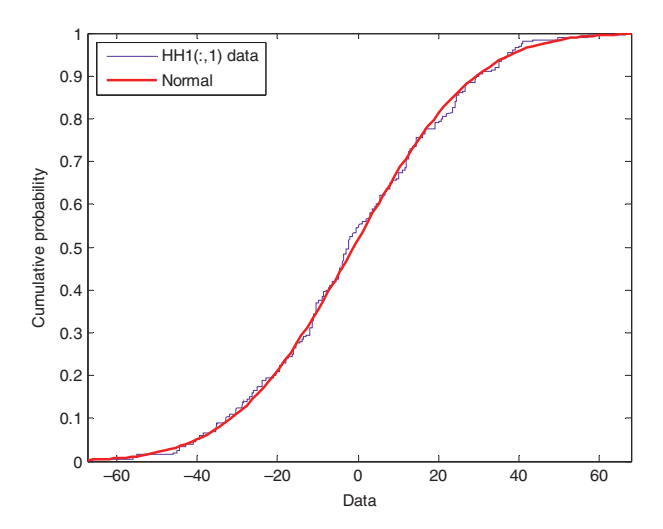


Figure 5: Cumulative Distribution Plot for HH Sub-band.

wavelet coefficients in the HH sub-band in level 1 and the corresponding fitting of Gaussian distribution are shown in Figure 5.

2.2 MMSE Estimator

This section discusses the proposed MMSE estimator. The MMSE estimator is used to retrieve the noise-free coefficients, assuming the coefficients are distributed by a suitable prior. The problem is retrieving the noise-free coefficients from the noisy image. Let the estimation of $x_k^l(i,j)$ be $\hat{x}_k^l(i,j)$. The problem is to minimize the mean squared error (mse) between the true and estimated data. mse is given by

$$\operatorname{mse}(\hat{x}_{k}^{l}(i,j), x_{k}^{l}(i,j)) = \frac{1}{M^{2}} ||\hat{x}_{k}^{l}(i,j) - x_{k}^{l}(i,j)||^{2} = \frac{1}{M^{2}} \sum_{i,j=1}^{M} (\hat{x}_{k}^{l}(i,j) - x_{k}^{l}(i,j))^{2},$$
 (5)

where *M* is the size of image given by product of rows and columns of image.

Due to the orthogonality property of DWT, the wavelet-transformed additive noise can be approximated by Gaussian distribution with mean = 0 and variance $\hat{\sigma}_n^2$. The MMSE estimator for the wavelet coefficients of the true image is a linear function and is given by Eq. (6):

$$\hat{x}_{k}^{l}(i,j) = \frac{\hat{\sigma}_{x}^{2}}{\hat{\sigma}_{x}^{2} + \hat{\sigma}_{n}^{2}} y_{k}^{l}(i,j), \tag{6}$$

where $\hat{\sigma}_{x}^{2}$ is the estimated variance of true wavelet coefficients and $\hat{\sigma}_{n}^{2}$ is the estimated variance of the additive noise.

2.3 Estimation of Signal and Noise Variances

Estimation of the variance is the most important step in the de-noising technique, based on statistical modeling of wavelet coefficients. The MMSE estimator depends upon the quality of the estimation of $\hat{\sigma}_x^2$ and $\hat{\sigma}_n^2$. The estimation of true wavelet coefficients needs information of the variances $\hat{\sigma}_x^2$ and $\hat{\sigma}_n^2$. An MLE is used to find the parameters of NIG PDF in a sub-band. The statistical properties of the transformed coefficients are modeled to estimate the variance. Local data statistics play an important role in the estimation of signal parameters α and δ . It is assumed that the coefficients in a sub-band form a vector. The maximum likelihood estimate for $\hat{\alpha}$ and $\hat{\delta}$ can be approximated by using the Hermite–Gauss quadrature rule and given by

$$\hat{\alpha} = \arg\max_{\alpha} \sum_{n=1}^{M_b} \ln\left(\left(\frac{1}{\sqrt{\pi}}\right) \sum_{s=1}^{R} w_s p_x \left((y(n) - \sqrt{2}\sigma_n x_s)\right)\right),\tag{7}$$

$$\hat{\delta} = \arg\max_{\delta} \sum_{n=1}^{M_b} \ln\left(\left(\frac{1}{\sqrt{\pi}}\right) \sum_{s=1}^{R} w_s p_x \left((y(n) - \sqrt{2}\sigma_n x_s)\right)\right),\tag{8}$$

where M_b = size of the sub-band, R = order of Hermite polynomial, x_s = root of Hermite polynomial, and w_s = weight of the root.

Using the estimated value of signal parameters, the signal variance $\hat{\sigma}_{x}^{2}$ is calculated and is given by [25]

$$\hat{\sigma}_{x}^{2} = \int_{-\infty}^{+\infty} x^{2} \hat{p}_{x}(x) dx - \left(\int_{-\infty}^{+\infty} x \hat{p}_{x}(x)\right)^{2}$$

$$= \sum_{x} x^{2} \hat{p}_{x}(x) - \left(\sum_{x} x \hat{p}_{x}(x)\right)^{2} \text{ (for discrete random variable } X\text{),}$$
(9)

where $\hat{p}_x(x)$ is the NIG PDF taking $\hat{\alpha}$ and $\hat{\delta}$ as distribution parameters and defined by Eq. (4). To estimate the Gaussian noise variance $\hat{\sigma}_n^2$, a median estimator is used [27]:

$$\hat{\sigma}_n^2 = \left(\frac{\text{Median}(y_k^I(i,j))}{0.6745}\right)^2,\tag{10}$$

where l=3 and k=3.

3 Proposed De-noising Algorithm

This section discusses the de-noising algorithm for removing additive noise in MR images. In the proposed method, the input noisy image is first converted to wavelet sub-bands by applying wavelet transform. Wavelet sub-bands consist of wavelet coefficients. Further wavelet coefficients are statistically modeled by NIG and Gaussian PDFs, and processed by MLE and MAD estimators. By utilizing the dependency between the wavelet coefficients, the signal and noise information are collected. The MMSE estimator utilizes the variance information of signal and noise, and calculates the shrinkage factor. The wavelet coefficients are shrunk by the

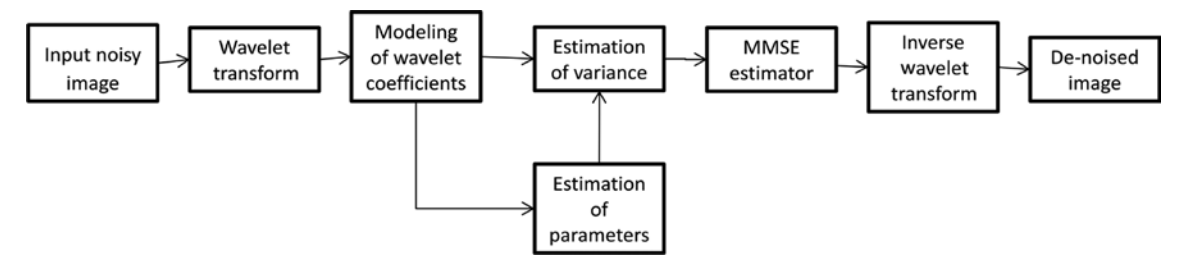


Figure 6: Block Diagram of Bayesian Multiresolution Approach for De-noising MR Image.

shrinkage factor. The resulting wavelet coefficients are then inverse wavelet transformed to obtain the desired de-noised image. Figure 6 shows the block diagram of the proposed Bayesian multiresolution approach for de-noising MR images. A detailed explanation of block diagram and summary of the proposed de-noising algorithm are discussed through the following steps.

- Step 1: Perform wavelet transform of the input noisy image, degraded by additive noise.
- Step 2: Model the wavelet coefficients using NIG PDF, generated in step 1.
- Step 3: By applying MLE, find the signal parameters $\hat{\alpha}$ and $\hat{\delta}$ using Eqs. (7) and (8), respectively.
- Step 4: Find the signal and noise variances using Eqs. (9) and (10), respectively.
- Step 5: Obtain the modified wavelet coefficients applying the MMSE estimator given in Eq. (6).
- Step 6: Carry out inverse wavelet transform to reconstruct the noise-free image.

4 Simulation Results

Simulation is carried out using an MR image of size 400×400 [32]. A three-level DWT using Daubechies 8 (db8) wavelet is carried out to decompose the MRI. Qualitative and quantitative comparisons are performed, to evaluate the effectiveness of the proposed method. The performance and quality parameters of the proposed method are compared with Donoho's soft thresholding [15], Bayes Shrink [10], and method in Ref. [8]. Figure 7 shows a qualitative comparison of the proposed method and state-of-the-art methods. It can be noticed that the proposed algorithm has the best visual quality compared with the other compared methods. The comparison of the proposed method and state-of-the-art methods in terms of peak signal-to-noise ratio (PSNR), structure similarity index (SSIM), Pratt's figure of merit (pratt-FOM) [18], Bhattacharyya coefficient (BC) [38], mean squared difference (MSD) [35], and signal-to-noise ratio (SNR) is given in Tables 1–6, respectively. PSNR is the performance evaluation parameter. SSIM and BC are the similarity measures. The maximum value in SSIM and BC shows high similarity between the measured quantities. pratt-FOM is the edge preservation parameter. It shows the edge preservation accuracy by obtaining the displacement between the detected edge location and ideal edge location. A high value of pratt-FOM indicates less difference between the detected and actual edge points. The value varies between 0 and 1, for SSIM, pratt-FOM, and BC parameters. MSD shows the degree of dissimilarity. A high value of MSD shows less similarity, and less value shows high similarity between the measured quantities and pixel intensities. SNR is a performance parameter and is defined as the ratio of signal power to noise power. A high value of SNR is required for better results. The comparison parameters are discussed as follows.

(i) The PSNR is defined as

PSNR =
$$20 \log_{10} \frac{255}{\sqrt{\text{mse}}}$$
, (11)

where mse is defined as

$$mse = \frac{1}{m \times n} \sum_{i=1}^{m \times n} (\hat{y}(i,j) - y(i,j))^{2}.$$
 (12)

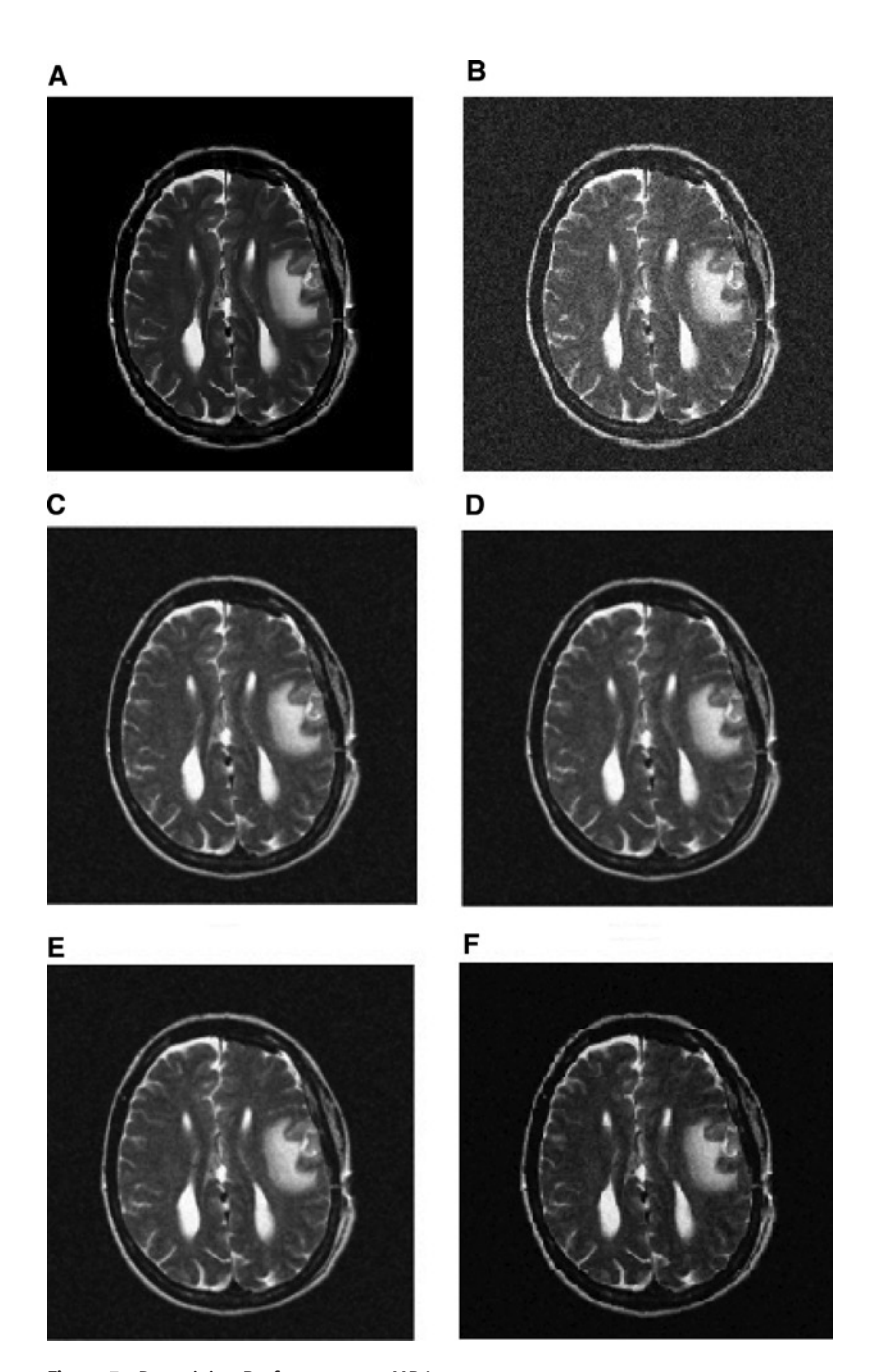


Figure 7: De-noising Performance on MR Image. (A) Ground truth. (B) Ground truth image corrupted with white Gaussian noise with σ_η = 0.3. (C) Image de-noising using Donoho's soft threshold. (D) Image de-noising using Bayes Shrink. (E) Image de-noising using method in Ref. [8]. (F) Image de-noising using the proposed method.

Table 1: Comparison of PSNR (dB) Performance for MR Images.

Method	Noise standard devia					
	0.1	0.2	0.3	0.4	0.5	
Donoho's soft threshold [15]	33.39	29.68	26.35	24.17	22.40	
Bayes Shrink [10]	34.22	30.54	28.49	26.23	24.87	
Bhuiyan et al. [8]	36.61	32.49	31.71	30.05	28.26	
Proposed method	40.16	36.25	34.60	33.02	31.87	

(ii) The SSIM is the quality assessment parameter and shows the similarity between two images. SSIM is given by

$$SSIM = (2\overline{y(i,j)}\hat{y}(i,j) + 2.55)(2\sigma_{y\hat{y}} + 7.65) / (\overline{y(i,j)}^2 + \overline{\hat{y}(i,j)}^2 + 2.55)(\sigma_y^2 + \sigma_{\hat{y}}^2 + 7.65),$$
(13)

where, y(i,j) and $\overline{\hat{y}(i,j)}$ are the expectation of input and recovered image, respectively. $\sigma_{\hat{y}}$ is the covariance information between input and recovered image. $\sigma_{\hat{y}}^2$ and $\sigma_{\hat{y}}^2$ are the variance of input and recovered image, respectively. For good visual quality, a unit value of SSIM is required.

(iii) The pratt-FOM is defined as

FOM =
$$(1/\max(I_o, I_D))\sum_{j=1}^{I_D} \frac{1}{1+\alpha D^2}$$
, (14)

where D is the difference between the original image edge points and detected image edge points. I_o is the number of edge points in the original image. I_D is the number of edge points in the detected image. α is the scaling constant and usually taken as a value of 1/9.

(iv) The BC is defined as

$$BC = e^{\left[-\frac{1}{2N}\ln\left(\frac{|E|}{\sqrt{|Q^TC_DQ||Q^TC_DQ|}}\right)\right]},$$
(15)

where C_o is the covariance matrix of original image matrix and C_D is the covariance matrix of detected image matrix.

$$Q = \left(\frac{C_o + C_D}{2}\right). \tag{16}$$

E is the diagonal matrix containing the eigenvalues of *Q* and *N* is the number of modes required to capture 90% variance of *Q*.

(v) The MSD is defined as

$$MSD = \overline{(\hat{y}(i,j) - y(i,j))^2}, \tag{17}$$

where, (\bar{.}) denote the expected value.

(vi) The SNR is defined as

SNR =
$$10 \log_{10} \left[\frac{\sum_{i=1}^{m \times n} y(i,j)^2}{\sum_{i=1}^{m \times n} (\hat{y}(i,j) - y(i,j))^2} \right].$$
 (18)

It is observed that the proposed method gains better PSNR, SSIM, pratt-FOM, BC, MSD, and SNR value irrespective of the noise parameter. The proposed approach is based on a multiresolution approach. Compared to other transform techniques, DWT provides a powerful tool for removing noise from the image. Daubechies wavelet defines the scaling signals and wavelets using more values from the signal. This feature provides great improvement in image enhancement. One of the most important properties of Daubechies wavelet transform is that it conserves the energy of signal, thus reducing the losses and improving the denoising efficiency. All noise and signal parameters and shrinkage factor are estimated using Bayesian estimators. The Bayes approach is based on prior knowledge. NIG PDF and Gaussian PDF are used as priors to find the signal and noise data. HH sub-band contains most of the noise information. Thus, this sub-band is modeled using Gaussian PDF to obtain the correct noise variance information. Knowledge of the suitable prior has a great role in de-noising performance. It is clearly shown in Figures 3, 4, and 5 that the proposed

PDFs correctly model the wavelet coefficients in different sub-bands. The obtained results from Tables 1-6 validate the choice of PDFs, and hence the effectiveness of the proposed method. Thus, wavelet transform in the Bayesian environment works effectively to reduce noise from MR image.

Table 2: Comparison of SSIM Performance for MR Images.

Method			Noise standard	Noise standard deviation (σ_{η})	
	0.1	0.2	0.3	0.4	0.5
Donoho's soft threshold [15]	0.9423	0.9261	0.9175	0.8941	0.8792
Bayes shrink [10]	0.9668	0.9479	0.9393	0.9311	0.9168
Bhuiyan et al. [8]	0.9781	0.9685	0.9466	0.9478	0.9249
Proposed method	0.9983	0.9719	0.9612	0.9560	0.9431

Table 3: Comparison of Pratt-FOM Performance for MR Images.

Method		deviation (σ_{η})			
	0.1	0.2	0.3	0.4	0.5
Donoho's soft threshold [15]	0.8032	0.7954	0.7668	0.7307	0.7418
Bayes Shrink [10]	0.9165	0.8863	0.8778	0.8651	0.8125
Bhuiyan et al. [8]	0.9324	0.9298	0.9221	0.9119	0.9009
Proposed method	0.9985	0.9892	0.9730	0.9654	0.9571

Table 4: Comparison of BC Performance for MR Images.

Method	Noise standard devia				
	0.1	0.2	0.3	0.4	0.5
Donoho's soft threshold [15]	0.3761	0.3578	0.3363	0.3222	0.3136
Bayes Shrink [10]	0.4974	0.4736	0.4532	0.4361	0.4229
Bhuiyan et al. [8]	0.5415	0.5194	0.5055	0.4972	0.4936
Proposed method	0.7819	0.7530	0.7357	0.7267	0.6929

Table 5: Comparison of MSD Performance for MR Images.

Method				Noise standard deviation (σ_η)	
	0.1	0.2	0.3	0.4	0.5
Donoho's soft threshold [15]	0.000667	0.000732	0.000884	0.000943	0.001044
Bayes Shrink [10]	0.000355	0.000410	0.000479	0.000529	0.000765
Bhuiyan et al. [8]	0.000342	0.000395	0.000464	0.000491	0.000582
Proposed method	0.000324	0.000377	0.000441	0.000474	0.000529

Table 6: Comparison of SNR (dB) Performance for MR Images.

Method		Noise standard	deviation (σ_{η})		
	0.1	0.2	0.3	0.4	0.5
Donoho's soft threshold [15]	19.60	16.88	15.80	12.47	10.04
Bayes Shrink [10]	20.35	17.38	16.57	15.55	12.74
Bhuiyan et al. [8]	23.69	18.81	18.20	17.27	16.19
Proposed method	25.10	22.90	20.47	19.39	18.78

Table 7: Comparison of De-noising Algorithms in Terms of Computational Time.

Method	Time (s)
Donoho's soft threshold [15]	1.46
Bayes Shrink [10]	3.43
Bhuiyan et al. [8]	4.91
Proposed method	4.12

Referring to Table 1, it can be observed that the proposed method gains the highest value of PSNR (dB). It is 40.16 for noise standard deviation (σ) of 0.1, which is more than the required PSNR for medical images. The improvement of PSNR of the proposed method is 16.85%, 14.79%, and 8.83% over Donoho's soft thresholding, Bayes Shrink, and method in Ref. [8], respectively. Table 2 shows the SSIM parameters for different de-noising methods. The SSIM of the proposed method is 0.9983, 0.9719, 0.9612, 0.9560, and 0.9431 for noise standard deviation of 0.1, 0.2, 0.3, 0.4, and 0.5, respectively. The SSIM of the proposed method is closer to 1 than that of the other tested methods. The improvement of SSIM of the proposed method is 5.61%, 3.15%, and 2.02% over Donoho's soft thresholding, Bayes Shrink, and method in Ref. [8], respectively, for noise standard deviation of 0.1. Table 3 shows the comparison of pratt-FOM for different de-noising methods. The proposed method achieves good improvement in edge preservation, which is a desirable property in high-resolution images. For noise standard deviation of 0.1, the pratt-FOM improvement of the proposed method is 19.55%, 8.21%, and 6.61% over Donoho's soft thresholding, Bayes Shrink, and method in Ref. [8], respectively. Table 4 shows the measured values of BC for different de-noising methods. The improvement of BC of the proposed method is 51.89%, 36.38%, and 30.74% over Donoho's soft thresholding, Bayes Shrink, and method in Ref. [8], respectively, for noise standard deviation of 0.1. This shows the effectiveness of the proposed method in terms of similarity measures. From Table 5, it can be seen that the lowest value of MSD is 0.000324 ($\sigma_{ij} = 0.1$) for the proposed method, and it can be concluded that the degree of dissimilarity of the proposed method is less than that of other state-of-the-art methods. Table 6 shows the SNR for the proposed and state-of-the-art methods. The SNR improvement of the proposed method is 5.61%, 17.86%, 11.08%, 12.27%, and 13.79% over the next best method for noise standard deviation of 0.1, 0.2, 0.3, 0.4, and 0.5, respectively. This demonstrates the effectiveness of the proposed method for suppression of white Gaussian noise.

The comparison of de-noising algorithm in terms of computational time is shown in Table 7. The denoising methods were run using 1.70-GHz Intel Core i3 processor with $\sigma_n = 0.3$. The run time of the proposed method is better than the method proposed in Ref. [8] with the exception of Donoho's soft threshold [15] and Bayes Shrink [10] methods. The computation time of the proposed method was reduced by 16% compared with the method proposed in Ref. [8]. However, the proposed method is still recognized as a fast method.

A high value of the SNR parameter proves the effectiveness of the proposed method in reducing Gaussian noise from MR images. The proposed algorithm is simple and computationally less complex.

5 Conclusion

The authors have proposed a de-noising method based on multiresolution and Bayesian approaches. A normal inverse Gaussian probability distribution function was used to model the wavelet coefficients. Modeled coefficients were analyzed by use of MLE to obtain the signal parameters and hence the signal variance. Noise variance was estimated using a median estimator in diagonal sub-bands. The proposed method was able to suppress the additive noise, while keeping the structure of the MR image unaltered. The algorithm simulated on the MR image showed that the combination of the Bayesian approach estimator and multiresolution approach is efficient and easier to implement.

We would like to further evaluate the performance of the method for Rician distributed noise, which will be reported in a future communication.

Acknowledgments: The authors are sincerely thankful to the anonymous reviewers for their critical comments and suggestions to improve the quality of the paper.

Bibliography

- [1] S. Aja-Fernandez, T. Pie and G. Vegas-Sanchez-Ferrero, Spatially variant noise estimation in MRI: a homomorphic approach, Med. Image Anal. 20 (2015), 184-194.
- [2] C. S. Anand and J. S. Sahambi, Wavelet domain non-linear filtering for MRI denoising, Magn. Reson. Imaging 28 (2010),
- [3] S. Anil, S. S. Sivaraju and N. Devarajan, A new contourlet based multiresolution approximation for MRI image noise removal, Natl. Acad. Sci. Lett. 40 (2017), 39-41.
- [4] S. P. Awate and R. T. Whitaker, Feature-preserving MRI denoising: a nonparametric empirical Bayes approach, IEEE Trans. Med. Imaging 26 (2007), 1242-1255.
- [5] P. Bao and L. Zhang, Noise reduction for magnetic resonance images via adaptive multiscale products thresholding, IEEE Trans. Med. Imaging 22 (2003), 1089–1099.
- [6] O. E. Barndorff-Nielsen, Normal inverse Gaussian distributions and stochastic volatility modelling, Scand. J. Stat. 24 (1997),
- [7] H. S. Bhadauria and M. L. Dewal, Medical image denoising using adaptive fusion of curvelet transform and total variation, Comput. Electr. Eng. 39 (2013), 1451-1460.
- [8] M. I. H. Bhuiyan, M. O. Ahmad and M. N. S. Swamy, A new method for denoising of images in the dual tree complex wavelet domain, in: IEEE North-East Workshop on Circuit and Systems, pp. 33-66, IEEE, Gatineau, Que., Canada, 2006.
- [9] M. I. H. Bhuiyan, M. O. Ahmad and M. N. S. Swamy, Wavelet based image denoising with the normal inverse Gaussian prior and linear MMSE estimator, IET Image Processing 2 (2008), 203-217.
- [10] S. G. Chang, B. Yu and M. Vetterli, Adaptive wavelet thresholding for image denoising and compression, IEEE Trans. Image Process. 9 (2000), 1532-1546.
- [11] Y. P. Chang, M. C. Hung, H. U. I. M. E. I. Liu and J. F. Jan, Testing symmetry of a NIG distribution, Commun. Stat.-Simul. C. 34 (2005), 851-862.
- [12] Y. Chen, Z.-C. Ji and C.-J. Hua, Efficient statistical modeling of wavelet coefficients for image denoising, Int. J. Wavelets Multiresolut. Inf. Process. 7 (2009), 629-641.
- [13] P. Coupe, J. V. Manjon, E. Gedamu, D. Arnold, M. Robles and D. L. Collins, Robust Rician noise estimation for MR images, Med. Image Anal. 14 (2010), 483-493.
- [14] K. Dabov, A. Foi, V. Katkovnik and K. Egiazarian, Image denoising by sparse 3-D transform-domain collaborative filtering, IEEE Trans. Image Process. 16 (2007), 2080-2095.
- [15] D. L. Donoho, De-noising by soft-thresholding, *IEEE Trans. Inf. Theory* **41** (1995), 613–627.
- [16] S. Gai, G. Yang, M. Wan and L. Wang, Hidden Markov tree model of images using quaternion wavelet transform, Comput. Electr. Eng. 40 (2014), 819-832.
- [17] S. Gai, Y. Zhang, C. Yang, L. Wang and J. Zhou, Color monogenic wavelet transform for multichannel image denoising, Multidimens. Syst. Signal Process. 28 (2017), 1463-1480.
- [18] C. I. Gonzalez, J. R. Castro, P. Melin and O. Castillo, Cuckoo search algorithm for the optimization of type-2 fuzzy image edge detection systems, in: 2015 IEEE Congress on Evolutionary Computation (CEC), pp. 449-455, IEEE, Sendai, Japan, 2015.
- [19] H. Gudbjartsson and S. Patz, The Rician distribution of noisy MRI data, Magn. Reson. Med. 34 (1995), 910-914.
- [20] G. Hamarneh and J. Hradsky, Bilateral filtering of diffusion tensor magnetic resonance images, IEEE Trans. Image Process. **16** (2007), 2463-2475.
- [21] L. He and I. R. Green Shields, A nonlocal maximum likelihood estimation method for Rician noise reduction in MR images, IEEE Trans. Med. Imaging 28 (2009), 165-172.
- [22] K. Kagoiya and E. Mwangi, A hybrid and adaptive non-local means wavelet based MRI denoising method with bilateral filter enhancement, Int. J. Comput. Appl. 166 (2017), 1-7.
- [23] M. Kivanc Mihcal, I. Kozintsev, K. Ramchandran and P. Moulin, Low-complexity image denoising based on statistical modeling of wavelet coefficients, IEEE Signal Process. Lett. 6 (1999), 300-303.
- [24] K. Krissian and S. Aja-Fernandez, Noise-driven anisotropic diffusion filtering of MRI, IEEE Trans. Image Process. 18 (2009), 2265-2274.
- [25] A. Leon-Garcia, Probability, Statistics, and Random Processes for Electrical Engineering, 3rd ed., Prentice Hall, New Jersey, USA, 2007.
- [26] A. Macovski, Noise in MRI, Magn. Reson. Med. 36 (1996), 494-497.
- [27] S. Mallat, A theory for multiresolution signal decomposition: the wavelet representation, IEEE Trans. Pattern Anal. Mach. Intell. 11 (1989), 674-693.
- [28] J. V. Manjon, M. Robles and N. A. Thacker, Multispectral MRI de-noising using non-local means, in: Proceedings of Medical Image Understanding and Analysis (MIUA), Aberystwyth, Wales, pp. 41–46, 2007.

- [29] J. V. Manjon, P. Coupe, L. Marti-Bonmati, D. L. Collins and M. Robles, Adaptive non-local means denoising of MR images with varying noise levels, J. Magn. Reson. Imaging 31 (2010), 192-203.
- [30] E. R. Mcveigh, R. M. Henkelman and M. J. Bronskill, Noise and filtration in magnetic resonance imaging, Med. Phys. 12 (1985), 586-591.
- [31] J. Mohan, V. Krishnaveni and Y. Guo, A survey on the magnetic resonance image denoising methods, Biomed. Signal Process. Control 9 (2004), 56-69.
- [32] Osirix, OSIRIX DICOM image library, [ONLINE] Available at: http://www.osirix-viewer.com/resources/diacom-imagelibrary/, 2014, Accessed 14 May, 2017.
- [33] J. Rajan, J. Arnold and J. Sijbers, A new non-local maximum likelihood estimation method for Rician noise reduction in magnetic resonance images using the Kolmogorov-Smirnov test, Signal Process. 103 (2014), 16-23.
- [34] T. W. Redpath, Signal-to-noise ratio in MRI, Br. J. Radiol. 71 (1998), 704–707.
- [35] U. Shardanand and P. Maes, Social information filtering: algorithms for automating "world of mouth," in: Proceedings of the SIGCHI Conference on Human Factors in Computing Systems, pp. 210-217, ACM Press/Addition Wesley Publishing Co., Denver, Colorado, USA, 1995.
- [36] J. Sijbers and A. J. Den Dekker, Maximum likelihood estimation of signal amplitude and noise variance from MR data, Magn. Reson. Med. 51 (2004), 586-594.
- [37] J. Sijbers, A. J. Den Dekker, J. Van Audekerke, M. Verhoye and D. van Dyck, Estimation of the noise in magnitude MR images, Magn. Reson. Imaging 16 (1998), 87-90.
- [38] L. Skjaerven, X. Q. Yao, G. Scarabelli and B. J. Grant, Integrating protein structural dynamics and evolutionary analysis with BIO3D, BMC Bioinformatics 15 (2014), 399.
- [39] Z. Wu Q., J. A. Ware and J. Jiang, Wavelet-based Rayleigh background removal in MRI, Electron. Lett. 39 (2003), 603-604.
- [40] S. Zaroubi and G. Goelman, Complex denoising of MR data via wavelet analysis: application for functional MRI, Magn. Reson. Imaging 18 (2000), 59-68.
- [41] H. Zhu, Y. Li, J. G. Ibrahim, X. Shi, H. An, Y. Chen, W. Gao, W. Lin, D. B. Rowe and B. S. Peterson, Regression models for identifying noise sources in magnetic resonance images, J. Am. Stat. Assoc. 104 (2009), 623-637.